Appl. Math. Mech. -Engl. Ed., **41**(12), 1881–1896 (2020)

APPLIED MATHEMATICS AND MECHANICS (ENGLISH EDITION)

https://doi.org/10.1007/s10483-020-2694-6

Subharmonic resonance of a clamped-clamped buckled beam with 1:1 internal resonance under base harmonic excitations*

Junda LI, Jianliang HUANG†

Department of Applied Mechanics and Engineering, Sun Yat-sen University, Guangzhou 510275, China

(Received Feb. 4, 2020 / Revised Oct. 19, 2020)

Abstract The subharmonic resonance and bifurcations of a clamped-clamped buckled beam under base harmonic excitations are investigated. The nonlinear partial integro-differential equation of the motion of the buckled beam with both quadratic and cubic nonlinearities is given by using Hamilton's principle. A set of second-order nonlinear ordinary differential equations are obtained by spatial discretization with the Galerkin method. A high-dimensional model of the buckled beam is derived, concerning nonlinear coupling. The incremental harmonic balance (IHB) method is used to achieve the periodic solutions of the high-dimensional model of the buckled beam to observe the nonlinear frequency response curve and the nonlinear amplitude response curve, and the Floquet theory is used to analyze the stability of the periodic solutions. Attention is focused on the subharmonic resonance caused by the internal resonance as the excitation frequency near twice of the first natural frequency of the buckled beam with/without the anti-symmetric modes being excited. Bifurcations including the saddle-node, Hopf, period-doubling, and symmetry-breaking bifurcations are observed. Furthermore, quasi-periodic motion is observed by using the fourth-order Runge-Kutta method, which results from the Hopf bifurcation of the response of the buckled beam with the anti-symmetric modes being excited.

Key words nonlinear vibration, buckled beam, incremental harmonic balance method, bifurcation, subharmonic resonance

Chinese Library Classification O322
2010 Mathematics Subject Classification 74K10

1 Introduction

As basic structural elements, buckled beams, whose dynamic equations consist of both quadratic and cubic nonlinearities, have been investigated for several decades. They can be found in airplanes, rockets, missiles, buildings in cold regions, foundations of heavy-duty machines, and micro-electromechanical systems (MEMS)[1]. Different methods have been applied

* Citation: LI, J. D. and HUANG, J. L. Subharmonic resonance of a clamped-clamped buckled beam with 1:1 internal resonance under base Harmonic excitations. *Applied Mathematics and Mechanics* (*English Edition*), **41**(12), 1881–1896 (2020) https://doi.org/10.1007/s10483-020-2694-6

† Corresponding author, E-mail: huangjl@mail.sysu.edu.cn

Project supported by the National Natural Science Foundation of China (Nos. 11972381 and 11572354) and the Fundamental Research Funds for the Central Universities (No. 18lgzd08)

in the nonlinear analysis of beams. Tseng and Dugundji[2] used the harmonic balance method to obtain the periodic responses of a clamped-clamped buckled beam. Abou-Rayan et al.[3] used the multiple-scale method to study the response of a simply-supported buckled beam under harmonic axial load, and found complicated dynamic behaviors including period-doubling response and chaos. Ibrahim et al.[4] used the shooting method, combined with the Newmark algorithm and the arc length continuation algorithm, to solve the periodic solutions of curved beams under periodic excitation. Ding et al.[5] investigated the responses of a viscoelastic beam under periodic excitation by using the harmonic balance method combined with the pseudo arc-length method, and showed the great difference in the nonlinear dynamics of the beam between rigid support and spring support. Fraternali et al.[6] focused on the nonlinear dynamics of curved composite beams, and presented a nonlinear layer-wise finite element model to describe the rotations of the cross-sections and strains and different elastic responses of the material. Huang et al.[7] used the incremental harmonic balance (IHB) method to study the nonlinear vibrations of a curved beam subjected to harmonic base excitation, and found complicated nonlinear responses including quasi-periodic response and chaos. Wang[8] investigated the weakly forced vibration of an axially moving viscoelastic beam, derived the nonlinear equations governing the transverse vibration, and used the Routh-Hurwitz criterion to examine the response stability. Wang et al.[9] used a new kinematic frame of the beam and continuum mechanics theory to analyze an axially accelerating beam, and utilized the multiple-scale method to get the steady-state frequency responses.

Internal resonance is a phenomenon that may happen when the ratio between two natural frequencies of a multiple-degree-of-freedom system is approximately an integer. The occurrence of internal resonance usually indicates the exchange of energy between two vibrational modes through the nonlinear coupling. Emam and Nayfeh[10] investigated the nonlinear response of a clamped-clamped buckled beam under primary resonance excitation, and found that single-mode response could raise a significant error in the dynamic analysis. In their later research[11], 1:1 internal resonance between the first and second modes and 3:1 internal resonance between the first and third modes were investigated. It was found that the period-doubling bifurcations led to chaos and chaotically amplitude-modulated response. Lee et al.[12] examined the anti-symmetric mode vibration of a clamped-clamped buckled beam. Tien et al.[13–14] studied the vibration of shallow arches with 1:1 internal resonance and 1:2 internal resonance. Öz and Pakdemirli[15] used the multiple-scale method to investigate the 2:1 internal resonance of a simply-supported curved beam, and discussed the steady-state solution, stability, and bifurcation. Huang et al.[16] investigated the nonlinear vibration of a simply-supported curved beam with 1:1 internal resonance between the first and third modes subjected to the base harmonic excitation, and discussed various bifurcation phenomena and responses of symmetric and anti-symmetric modes. Xiong et al.[17] studied the nonlinear dynamics of a viscoelastic buckled beam with 2:1 internal resonance, and observed a double-jumping phenomenon. Mao et al.[18] investigated the local and global resonances of a super-critically axially moving beam with 3:1 internal resonance, and discussed the excitation effect on the internal resonance.

Subharmonic and superharmonic resonances are typical characteristics of nonlinear vibration systems. Subharmonic resonances happen at the response frequencies containing $1/n$ $(n = 2, 3, 4, \cdots)$ of the excitation frequency[19–21]. Yang et al.[22] investigated the subharmonic and superharmonic resonances of a bistable system, and found that the components of the response frequencies were complicated. Mao et al.[23] investigated the superharmonic resonance of a super-critical axially moving beam, and found a 3:1 internal resonance. Emam and Nayfeh[24] investigated the nonlinear response of a clamped-clamped buckled beam subjected to subharmonic resonance excitation, and found the chaos resulting from a series of period-doubling bifurcations. However, for some special initial deflections which could result in various internal resonances, their subharmonic and superharmonic resonances have not been discussed yet.

This work aims to investigate various bifurcation phenomena of subharmonic resonances for a buckled beam with 1:1 internal resonance under base harmonic excitation. Special initial deflection of the center of a buckled beam is chosen so that the natural frequencies of the first and second modes can be close to each other, and various bifurcations of the response of the buckled beam including saddle-node, Hopf, period-doubling, and symmetry-breaking bifurcations are achieved. The remaining part of this paper is organized as follows. The equation governing the motion of the buckled beam and the incremental harmonic balance (IHB) method are given in Section 2. In Section 3, the nonlinear frequency responses of the buckled beam subjected to different level magnitudes of excitation are considered, and the amplitude responses of two typical frequencies are discussed. Finally, the main conclusions are summarized in Section 4.

2 Problem formulation

2.1 Equation of motion

A clamped-clamped buckled beam under investigation is schematically depicted in Fig. 1, which is similar to the model in Ref. [10]. The harmonic base support motion can be expressed as $G(\widehat{t}) = G_0\cos(\widehat{\Omega}\widehat{t})$, where $\widehat{\Omega}$ is the excitation frequency, and the corresponding uniform base harmonic excitation to the beam in a non-inertial reference system is

$$-\rho A\frac{\partial^2 G(\widehat{t})}{\partial\widehat{t}^2} = \rho A G_0\widehat{\Omega}^2\cos(\widehat{\Omega}\widehat{t}) = \widehat{F}\cos(\widehat{\Omega}\widehat{t}), \tag{1}$$

where ρ is the beam density, A is the cross-sectional area of the beam, $\widehat{\Omega}$ is the excitation frequency, and $\widehat{F}$ is the excitation magnitude. The transverse vibration of a clamped-clamped buckled beam subjected to a longitudinal static load and a transverse harmonic load can be derived by using Hamilton's principle[10,25]. The kinetic energy T and the potential energy V of the beam are

$$T = \frac{\rho A}{2}\int_0^l \Big(\frac{\partial\widehat{w}}{\partial\widehat{t}}\Big)^2\mathrm{d}\widehat{x}, \tag{2}$$

$$V = V_{\mathrm{b}} + V_{\mathrm{a}} + V_{\mathrm{s}} = \int_0^l \frac{1}{2}EI\Big(\frac{\partial^2\widehat{w}}{\partial\widehat{x}^2}\Big)^2\mathrm{d}\widehat{x} - \int_0^l \frac{1}{2}\widehat{P}\Big(\frac{\partial\widehat{w}}{\partial\widehat{x}}\Big)^2\mathrm{d}\widehat{x} + \frac{EA}{8l}\Big(\int_0^l \Big(\frac{\partial\widehat{w}}{\partial\widehat{x}}\Big)^2\mathrm{d}\widehat{x}\Big)^2, \tag{3}$$

where $\widehat{w}(\widehat{x},\widehat{t})$ is the transverse displacement, and V_{b}, V_{a}, and V_{s} are the potential energy due to the bending, the axial force $\widehat{P}$, and the midplane stretching, respectively. Other properties of the beam include Young's modulus E, the length l, the width r, the thickness s, and the flexural rigidity EI. The equations of motion and the associated boundary conditions are derived by using the extended Hamilton's Principle

$$\delta\int_{T_1}^{T_2}(T - V + W_{\mathrm{nc}})\mathrm{d}\widehat{t} = 0, \tag{4}$$

where W_{nc} is the nonconservative work. The first variation of the nonconservative force is

$$\delta\int_{T_1}^{T_2} W_{\mathrm{nc}}\mathrm{d}\widehat{t} = \int_{T_1}^{T_2}\Big(q - \widehat{c}\frac{\partial\widehat{w}}{\partial\widehat{t}}\Big)\delta\widehat{w}\mathrm{d}\widehat{t}, \tag{5}$$

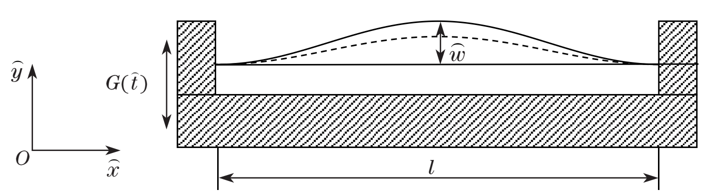

Fig. 1 Diagram of the clamped-clamped buckled beam subjected to base harmonic excitation

in which $q = \widehat{F}\cos(\widehat{\Omega}\widehat{t}\,)$ is the corresponding uniform base harmonic excitation to the beam, and $\widehat{c}$ is the damping factor. After some differential operations, the governing equation can be derived as follows:

$$\rho A \frac{\partial^2 \widehat{w}}{\partial \widehat{t}^{\,2}} + \widehat{P}\frac{\partial^2 \widehat{w}}{\partial \widehat{x}^{2}} + EI\frac{\partial^4 \widehat{w}}{\partial \widehat{x}^{4}} + \widehat{c}\frac{\partial \widehat{w}}{\partial \widehat{t}} = \frac{EA}{2l}\frac{\partial^2 \widehat{w}}{\partial \widehat{x}^{2}}\int_0^l \Big(\frac{\partial \widehat{w}}{\partial \widehat{x}}\Big)^2 \mathrm{d}\widehat{x} + \widehat{F}\cos(\widehat{\Omega}\widehat{t}\,). \tag{6}$$

For the clamped-clamped buckled beam, the boundary condition is

$$\widehat{w} = 0, \quad \frac{\partial \widehat{w}}{\partial \widehat{x}} = 0 \quad \text{at} \quad \widehat{x} = 0, l. \tag{7}$$

Using the following dimensionless variables:

$$w = \frac{\widehat{w}}{l}, \quad x = \frac{\widehat{x}}{l}, \quad t = \widehat{t}\sqrt{\frac{EI}{\rho A l^4}}, \quad \Omega = \widehat{\Omega}\sqrt{\frac{\rho A l^4}{EI}} \tag{8}$$

and substituting Eq. (8) into Eqs. (6) and (7) yield the nondimensional integro partial-differential equation as follows:

$$\ddot{w} + w^{\mathrm{iv}} + Pw'' + c\dot{w} - \alpha w''\int_0^1 {w'}^2 \mathrm{d}x = F\cos(\Omega t) \tag{9}$$

with the boundary conditions

$$w = 0 \quad \text{and} \quad w' = 0 \quad \text{at} \quad x = 0 \quad \text{and} \quad 1, \tag{10}$$

where the overdot of w indicates the derivative with respect to t, the prime indicates the derivative with respect to x, and

$$P = \frac{\widehat{P}l^2}{EI}, \quad \alpha = \frac{Al^2}{2I}, \quad c = \frac{\widehat{c}\,l^2}{\sqrt{\rho AEI}}, \quad F = \frac{\widehat{F}l^3}{EI}. \tag{11}$$

2.2 Buckling problem

Since it is not easy to get an accurate measurement of the axial force P, the relationship between the axial force and the initial transverse deflection is figured out in this section. By dropping the time derivatives and the dynamic load from Eqs. (9) and (10), one can obtain the following static equation:

$$w^{\mathrm{iv}} + Pw'' - \alpha w''\int_0^1 {w'}^2 \mathrm{d}x = 0, \tag{12}$$

$$w(0) = w(1) = w'(0) = w'(1) = 0. \tag{13}$$

The critical buckling load P_{c} and its buckling shape can be derived from the linearized form of Eq. (12). Following the derivation in Ref. [10], the lowest buckling mode shape and its corresponding buckling load are

$$\psi = \frac{1}{2}(1 - \cos(2\pi x)), \quad P_{\mathrm{c}} = 4\pi^2, \tag{14}$$

where ψ is normalized so that $\psi(1/2) = 1$.

Since the initial deflection is far smaller than the longitudinal length, the displacement of the buckled beam can be expressed as

$$w(x) = b\psi(x), \tag{15}$$

where b is the dimensionless initial deflection of the middle of the buckled beam. Substituting Eq. (15) into Eq. (12) yields

$$b^2 = \frac{P - P_{\mathrm{c}}}{\alpha} \int_0^1 \psi'^2 \mathrm{d}x. \tag{16}$$

To study the nonlinear vibrations around the buckled position, let the solution to Eq. (9) be

$$w(x,t) = b\psi(x) + v(x,t). \tag{17}$$

Then, $w(x)$ can be the sum of static deformation and dynamic deformation. Substituting Eqs. (16) and (17) into Eqs. (9) and (10) yields

$$\ddot{v} + v^{\mathrm{iv}} + P_{\mathrm{c}} v'' - \alpha(b\psi + v)'' \int_0^1 (2b\psi' v' + v'^2)\mathrm{d}x = F\cos(\Omega t), \tag{18}$$

$$v(0) = v(1) = v'(0) = v'(1) = 0. \tag{19}$$

Following Nayfeh et al.[26] to determine the linear vibration natural frequencies of the beam and their mode shapes and dropping the damping, forcing, and nonlinear terms yield

$$\ddot{v} + v^{\mathrm{iv}} + P_{\mathrm{c}} v'' - 2\alpha b^2 \psi'' \int_0^1 2v'\psi' \mathrm{d}x = 0. \tag{20}$$

Assume

$$v(x,t) = \Phi(x)\mathrm{e}^{\mathrm{i}\varpi t}, \tag{21}$$

where Φ and ϖ are the mode shape function and the natural frequency for any solution of the clamped-clamped buckled beam, respectively. Then, substituting Eq. (16) into Eq. (15) yields

$$\Phi^{\mathrm{iv}} + P_{\mathrm{c}}\Phi'' - \varpi^2\Phi = \alpha b^2 v'' \int_0^1 2\Phi' v' \mathrm{d}x. \tag{22}$$

The boundary conditions of the fixed-fixed buckled beam are

$$\Phi(0) = \Phi(1) = \Phi'(0) = \Phi'(1).$$

The general solution to Eq. (17) can be expressed as a linear combination of the homogeneous and particular solutions as follows:

$$\Phi(x,\varpi) = \Phi_h(x,\varpi) + \Phi_p(x,\varpi), \tag{23}$$

where

$$\Phi_h(x,\varpi) = c_1\sin(\lambda x) + c_2\cos(\lambda x) + c_3\sinh(\mu x) + c_4\cosh(\mu x), \tag{24}$$

$$\Phi_p(x,\varpi) = c_5\cos(2\pi x), \tag{25}$$

in which c_i $(i = 1, 2, 3, 4, 5)$ are constants.

Substituting Eqs. (18) and (20) into Eq. (17) yields

$$(b^4\pi^3\alpha - \varpi^2)c_5 = 2b^4\alpha\pi^3 \int_0^1 \Phi_h' \sin(2\pi x)\mathrm{d}x. \tag{26}$$

If $\int_0^1 \Phi_h' \sin(2\pi x)\mathrm{d}x = 0$, $c_5 = 0$ and the mode shapes are given by the homogeneous solution, i.e., the natural frequencies and their corresponding mode shapes (the symmetrical modes) are independent of the initial mid-span deflection b. If $\int_0^1 \Phi_h' \sin(2\pi x)\mathrm{d}x \neq 0$, $c_5 \neq 0$ and the eigenvalue problem yields the natural frequencies and their corresponding mode shapes (the anti-symmetrical modes) changing with the initial mid-span deflection b.

The transverse dynamic displacement $v(x,t)$ is assumed to be

$$v(x,t) = \sum_{j=1}^{n} Y_j(t)\phi_j(x), \tag{27}$$

where $\phi_j(x)$ $(j = 1, 2, 3, \cdots, n)$ are mode functions of the clamped-clamped buckled beam normalized, n is the number of modes under consideration, and $Y_j(t)$ $(j = 1, 2, 3, \cdots, n)$ are the generalized coordinates of the transverse vibration.

Substituting Eq. (27) into Eq. (18), multiplying all terms with $\phi_i(x)$, and integrating the resulting expression over the domain [0,1] yield

$$\begin{aligned}&\sum_{j=1}^{n} M_{ij}Y_i'' + \sum_{j=1}^{n} C_{ij}Y_i'' + \sum_{j=1}^{n} \widetilde{K}_{ij}Y_j + \sum_{j=1}^{n}\sum_{k=1}^{n} \widetilde{K}_{ijk}^{(2)}Y_jY_k + \sum_{j=1}^{n}\sum_{k=1}^{n}\sum_{l=1}^{n} \widetilde{K}_{ijkl}^{(3)}Y_jY_kY_l \\ &= f_i\cos(\Omega t), \quad i = 1, 2, 3, \cdots, n,\end{aligned} \tag{28}$$

where the prime of Y denotes differentiation with respect to t, and

$$\begin{cases} M_{ij} = \displaystyle\int_0^1 \phi_i\phi_j \mathrm{d}x, \quad C_{ij} = c\int_0^1 \phi_i\phi_j'' \mathrm{d}x, \\ \widetilde{K}_{ij} = \displaystyle\int_0^1 \phi_i\phi_j^{\mathrm{iv}}\mathrm{d}x + \int_0^1 P_{\mathrm{c}}\phi_i\phi_j''\mathrm{d}x - 2\alpha b^2\int_0^1 \phi_i\psi''\mathrm{d}x\int_0^1 \phi_j'\psi'\mathrm{d}x, \\ \widetilde{K}_{ijk}^{(2)} = -2\alpha b\displaystyle\int_0^1 \phi_i\phi_j''\mathrm{d}x\int_0^1 \psi'\phi_k'\mathrm{d}x - \alpha b\int_0^1 \phi_i\psi''\mathrm{d}x\int_0^1 \phi_j'\phi_k'\mathrm{d}x, \\ \widetilde{K}_{ijkl}^{(3)} = -\alpha\displaystyle\int_0^1 \phi_i\phi_j''\mathrm{d}x\int_0^1 \phi_k'\phi_l'\mathrm{d}x, \quad f_i = F\int_0^1 \phi_i\mathrm{d}x. \end{cases} \tag{29}$$

2.3 IHB method

The IHB method, originally developed by Lau and Cheung[27] and Cheung and Lau[28], provides a methodology for determining the periodic solutions of dynamical systems with general nonlinearities. The first step of the IHB method is an incremental method, which is a Newton-Raphson procedure to linearize the incremental differential equation of Eq. (28). Introduce

$$\tau = \omega t, \tag{30}$$

where ω is a fundamental frequency of a periodic response. Equation (28) can be written as

$$\begin{aligned}&\omega^2\sum_{j=1}^{n} M_{ij}\ddot{Y}_i + \omega\sum_{j=1}^{n} C_{ij}\dot{Y}_i + \sum_{j=1}^{n} \widetilde{K}_{ij}Y_j + \sum_{j=1}^{n}\sum_{k=1}^{n} \widetilde{K}_{ijk}^{(2)}Y_jY_k + \sum_{j=1}^{n}\sum_{k=1}^{n}\sum_{l=1}^{n} \widetilde{K}_{ijkl}^{(3)}Y_jY_kY_l \\ &= f_i\cos(\Omega t), \quad i = 1, 2, 3, \cdots, n,\end{aligned} \tag{31}$$

where the overdot of Y denotes differentiation with respect to the new time variable τ. Let Y_{i0}, f, and ω_0 denote a steady-state periodic solution. Then, a neighboring state can be expressed by adding increments to Y_{i0}, f, and ω_0 as follows:

$$Y_i = Y_{i0} + \Delta Y_i, \quad f_i = f_{i0} + \Delta f_i, \quad \omega = \omega_0 + \Delta\omega. \tag{32}$$

Substituting Eq. (32) into Eq. (31) and neglecting higher-order terms of the increments yield

$$\begin{aligned}&\omega_0^2\sum_{j=1}^{n}M_{ij}\Delta\ddot{Y}_i+\omega_0\sum_{j=1}^{n}C_{ij}\Delta\dot{Y}_i+\sum_{j=1}^{n}\Big(\widetilde{K}_{ij}+2\sum_{j=1}^{n}\sum_{k=1}^{n}\widetilde{K}_{ijk}^{(2)}Y_{k0}\\&+3\sum_{j=1}^{n}\sum_{k=1}^{n}\sum_{l=1}^{n}\widetilde{K}_{ijkl}^{(3)}Y_{k0}Y_{l0}\Big)\Delta Y_j\\=\ &R_i-\Delta\omega\sum_{j=1}^{n}(2\omega_0M_{ij}\ddot{Y}_{j0}+C_{ij}\dot{Y}_{j0})+\Delta f_i\cos(p\tau),\end{aligned}\tag{33}$$

where

$$\begin{aligned}R_i=\ &f_{i0}\cos(p\tau)-\Big({\omega_0}^2\sum_{j=1}^{n}M_{ij}\ddot{Y}_{i0}+\omega_0\sum_{j=1}^{n}C_{ij}\dot{Y}_{i0}+\sum_{j=1}^{n}\widetilde{K}_{ij}Y_{j0}+\sum_{j=1}^{n}\sum_{k=1}^{n}\widetilde{K}_{ijk}^{(2)}Y_{j0}Y_{k0}\\&+\sum_{j=1}^{n}\sum_{k=1}^{n}\sum_{l=1}^{n}\widetilde{K}_{ijkl}^{(3)}Y_{j0}Y_{k0}Y_{l0}\Big)\end{aligned}\tag{34}$$

is a correction term that vanishes if the result is the exact solution to the equations. Equations (33) and (34) can be rewritten in the matrix form as follows:

$$\omega_0^2\boldsymbol{M}\Delta\ddot{\boldsymbol{Y}}+\omega_0\boldsymbol{C}\Delta\dot{\boldsymbol{Y}}+(\boldsymbol{K}+2\boldsymbol{K}_2+3\boldsymbol{K}_3)\Delta\boldsymbol{Y}=\boldsymbol{R}-(2\omega_0\boldsymbol{M}\ddot{\boldsymbol{Y}}_0+\boldsymbol{C}\dot{\boldsymbol{Y}}_0)+\cos(p\tau)\Delta\boldsymbol{F},\tag{35}$$

where

$$\boldsymbol{R}=\boldsymbol{F}\cos(p\tau)-\Big(\omega_0^2\boldsymbol{M}\ddot{\boldsymbol{Y}}_0+\omega_0\boldsymbol{C}\dot{\boldsymbol{Y}}_0+(\boldsymbol{K}+\boldsymbol{K}_2+\boldsymbol{K}_3)\boldsymbol{Y}_0\Big)\tag{36}$$

is the correction vector.

The second step of the IHB method is a harmonic balance procedure. Under forced harmonic excitations, a periodic solution can be obtained by expanding Y_{j0} in a truncated Fourier series and using the Galerkin procedure. The solution can be assumed to have the following form:

$$Y_{j0}=\sum_{k=1}^{n_{\rm c}}a_{j,(k-1)/m}\cos\Big(\frac{k-1}{m}\tau\Big)+\sum_{k=1}^{n_{\rm s}}b_{j,k/m}\sin\Big(\frac{k}{m}\tau\Big)=\boldsymbol{C}_S\boldsymbol{A}_j,\tag{37}$$

where

$$\boldsymbol{C}_S=\Big(1\quad\cos\frac{\tau}{m}\quad\cos\frac{2\tau}{m}\quad\cdots\quad\cos\frac{(n_{\rm c}-1)\tau}{m}\quad\sin\frac{\tau}{m}\quad\sin\frac{2\tau}{m}\quad\cdots\quad\sin\frac{n_{\rm s}\tau}{m}\Big),\tag{38}$$

$$\boldsymbol{A}_j=\Big(a_{j,0}\quad a_{j,1/m}\quad a_{j,2/m}\quad\cdots\quad a_{j,(n_{\rm c}-1)/m}\quad b_{j,1/m}\quad b_{j,2/m}\quad\cdots\quad b_{j,n_{\rm s}/m}\Big)^{\rm T},\tag{39}$$

in which $a_{j,k/m}$ and $b_{j,k/m}$ are Fourier coefficients, and $n_{\rm c}$ and $n_{\rm s}$ are numbers of cosine and sine harmonic terms retained, respectively. The positive integer m can be set as a number larger than 1 if the system goes through period-doubling bifurcations. To ensure the accuracy, when $m=1$, $n_{\rm c}$ and $n_{\rm s}$ are chosen as 6 and 5 in this work, respectively. As for the period-m solution, one can choose $n_{\rm c}=1+5m$ and $n_{\rm s}=5m$. Then, Eq. (37) can be written as follows:

$$Y_{j0}=A_{j,0}+\sum_{k=1}^{5m}A_{j,k/m}\cos\Big(\frac{k}{m}\tau+\varphi_{j,k/m}\Big),\tag{40}$$

where

$$A_{j,k/m} = \sqrt{a_{j,k/m}^2 + b_{j,k/m}^2}, \quad \varphi_{j,k/m} = \arctan(-b_{j,k/m}, a_{j,k/m}). \tag{41}$$

The increment ΔY_j can also be expanded in a truncated Fourier series similar to Eq. (37) with $a_{j,k/m}$ and $b_{j,k/m}$ replaced by $\Delta a_{j,k/m}$ and $\Delta b_{j,k/m}$. Then, one can obtain

$$\Delta Y_{j0} = \boldsymbol{C}_S \Delta \boldsymbol{A}_j, \tag{42}$$

where

$$\Delta \boldsymbol{A}_j = (\Delta a_{j,0}\ \Delta a_{j,1/m}\ \Delta a_{j,2/m}\ \cdots\ \Delta a_{j,(n_c-1)/m}\ \Delta b_{j,1/m}\ \Delta b_{j,2/m}\ \cdots\ \Delta b_{j,n_s/m})^{\mathrm{T}}. \tag{43}$$

Hence, the vectors of generalized coordinates and their increments can be expressed by using the Fourier coefficient vector $\boldsymbol{A}$ and its increment $\Delta\boldsymbol{A}$ as follows:

$$\boldsymbol{Y}_0 = \boldsymbol{S}\boldsymbol{A}, \quad \Delta\boldsymbol{Y} = \boldsymbol{S}\Delta\boldsymbol{A}, \tag{44}$$

where

$$\boldsymbol{S} = \mathrm{diag}(\boldsymbol{C}_S,\, \boldsymbol{C}_S,\, \cdots,\, \boldsymbol{C}_S), \tag{45}$$

$$\boldsymbol{A} = (\boldsymbol{A}_1^{\mathrm{T}}\ \boldsymbol{A}_2^{\mathrm{T}}\ \cdots\ \boldsymbol{A}_n^{\mathrm{T}})^{\mathrm{T}}, \tag{46}$$

$$\Delta\boldsymbol{A} = (\Delta\boldsymbol{A}_1^{\mathrm{T}}\ \Delta\boldsymbol{A}_2^{\mathrm{T}}\ \cdots\ \Delta\boldsymbol{A}_n^{\mathrm{T}})^{\mathrm{T}}. \tag{47}$$

Differentiating Eq. (44) yields

$$\dot{\boldsymbol{Y}}_0 = \dot{\boldsymbol{S}}\boldsymbol{A}, \quad \Delta\dot{\boldsymbol{Y}} = \dot{\boldsymbol{S}}\Delta\boldsymbol{A}, \quad \ddot{\boldsymbol{Y}}_0 = \ddot{\boldsymbol{S}}\boldsymbol{A}, \quad \Delta\ddot{\boldsymbol{Y}} = \ddot{\boldsymbol{S}}\Delta\boldsymbol{A}. \tag{48}$$

Using the Galerkin procedure for one cycle in the harmonic balance process, Eq. (35) becomes

$$\begin{aligned}&\int_0^{2m\pi} \delta(\Delta\boldsymbol{Y})^{\mathrm{T}}(\omega_0^2\boldsymbol{M}\Delta\ddot{\boldsymbol{Y}} + \omega_0\boldsymbol{C}\Delta\dot{\boldsymbol{Y}} + (\boldsymbol{K} + 2\boldsymbol{K}_2 + 3\boldsymbol{K}_3)\Delta\boldsymbol{Y})\mathrm{d}\tau \\ =& \int_0^{2m\pi} \delta(\Delta\boldsymbol{Y})^{\mathrm{T}}(\boldsymbol{R} - (2\omega_0\boldsymbol{M}\ddot{\boldsymbol{Y}}_0 + \boldsymbol{C}\dot{\boldsymbol{Y}}_0) + \cos(p\tau)\Delta\boldsymbol{F})\mathrm{d}\tau.\end{aligned} \tag{49}$$

Substituting Eqs. (44)–(48) into Eq. (49) yields a set of linear equations in terms of $\Delta\boldsymbol{A}$ and $\Delta\omega$ as follows:

$$\overline{\boldsymbol{K}}_{mc}\Delta\boldsymbol{A} = \overline{\boldsymbol{R}} - \overline{\boldsymbol{R}}_\omega\Delta\omega + \overline{\boldsymbol{R}}_f\Delta\boldsymbol{F}, \tag{50}$$

where

$$\begin{cases}\overline{\boldsymbol{K}}_{mc} = \omega_0^2\overline{\boldsymbol{M}} + \omega_0\overline{\boldsymbol{C}} + \overline{\boldsymbol{K}} + 2\overline{\boldsymbol{K}}_2 + 3\overline{\boldsymbol{K}}_3, \\ \overline{\boldsymbol{R}} = \overline{\boldsymbol{F}} - (\omega_0^2\overline{\boldsymbol{M}} + \omega_0\overline{\boldsymbol{C}} + \overline{\boldsymbol{K}} + 2\overline{\boldsymbol{K}}_2 + 3\overline{\boldsymbol{K}}_3)\boldsymbol{A}, \quad \overline{\boldsymbol{R}}_\omega = (2\omega_0\overline{\boldsymbol{M}} + \overline{\boldsymbol{C}})\boldsymbol{A},\end{cases} \tag{51}$$

in which

$$\begin{cases}\overline{\boldsymbol{M}} = \displaystyle\int_0^{2m\pi}\boldsymbol{S}^{\mathrm{T}}\boldsymbol{M}\boldsymbol{S}''\mathrm{d}\tau, \quad \overline{\boldsymbol{C}} = \int_0^{2m\pi}\boldsymbol{S}^{\mathrm{T}}\boldsymbol{C}\boldsymbol{S}'\mathrm{d}\tau, \quad \overline{\boldsymbol{K}} = \int_0^{2m\pi}\boldsymbol{S}^{\mathrm{T}}\boldsymbol{K}\boldsymbol{S}\mathrm{d}\tau, \\ \overline{\boldsymbol{K}}_2 = \displaystyle\int_0^{2m\pi}\boldsymbol{S}^{\mathrm{T}}\boldsymbol{K}_2\boldsymbol{S}\mathrm{d}\tau, \quad \overline{\boldsymbol{K}}_3 = \int_0^{2m\pi}\boldsymbol{S}^{\mathrm{T}}\boldsymbol{K}_3\boldsymbol{S}\mathrm{d}\tau, \\ \overline{\boldsymbol{F}} = \displaystyle\int_0^{2m\pi}\boldsymbol{S}^{\mathrm{T}}\boldsymbol{F}\cos(p\tau)\mathrm{d}\tau, \quad \overline{\boldsymbol{R}}_f = \int_0^{2m\pi}\boldsymbol{S}^{\mathrm{T}}\cos(p\tau)\mathrm{d}\tau.\end{cases} \tag{52}$$

The solving process begins with a guessed solution. If $\boldsymbol{F}$ is fixed as a parameter vector, the frequency response curve can be found point-by-point by increasing the frequency ω or a component of the coefficient vector $\boldsymbol{A}$. If the frequency ω can be treated as a constant value, the amplitude response curve can be found by increasing the excitation magnitude f_i or a component of the coefficient vector $\boldsymbol{A}$. Each result can be found only when the norm of $\overline{\boldsymbol{R}}$ is smaller than 1.0×10^{-10} in this work.

2.4 Stability theory

After the steady-state periodic solution to the nonlinear equation has been calculated, its stability and bifurcation will then be considered. Adding a small perturbation ΔY_j to Y_{j0}, i.e.,

$$Y_j = Y_{j0} + \Delta Y_j. \tag{53}$$

Substituting Eq. (53) into Eq. (31) and noting that Y_{j0} satisfies Eq. (31) yield

$$\begin{aligned}&\omega^2 \sum_{j=1}^{n} M_{ij}\Delta\ddot{Y}_i + \omega\sum_{j=1}^{n} C_{ij}\Delta\dot{Y}_i + \sum_{j=1}^{n}\Big(\widetilde{K}_{ij} + 2\sum_{j=1}^{n}\sum_{k=1}^{n}\widetilde{K}^{(2)}_{ijk}Y_{k0}\\&+3\sum_{j=1}^{n}\sum_{k=1}^{n}\sum_{l=1}^{n}\widetilde{K}^{(3)}_{ijkl}Y_{k0}Y_{l0}\Big)\Delta Y_j = 0.\end{aligned} \tag{54}$$

Equation (54) can be written in the matrix form

$$\omega^2\boldsymbol{M}\Delta\ddot{\boldsymbol{Y}} + \omega\boldsymbol{C}\Delta\dot{\boldsymbol{Y}} + (\boldsymbol{K} + 2\boldsymbol{K}_2(\boldsymbol{Y}_0)+3\boldsymbol{K}_3(\boldsymbol{Y}_0))\Delta\boldsymbol{Y} = 0. \tag{55}$$

It is the perturbed equation from the known solution q_0. The stability of the periodic solution corresponds to the stability of the solution to Eq. (31).

Equation (55) can be rewritten in the state space form

$$\boldsymbol{X}' = \boldsymbol{Q}(\tau)\boldsymbol{X}, \tag{56}$$

where

$$\dot{\boldsymbol{X}} = (\Delta\boldsymbol{Y}\ \ \Delta\dot{\boldsymbol{Y}})^{\mathrm{T}}, \tag{57}$$

$$\boldsymbol{Q} = \begin{pmatrix} \boldsymbol{0} & \boldsymbol{I} \\ \boldsymbol{Q}_{21}(\tau) & \boldsymbol{Q}_{22}\end{pmatrix}, \tag{58}$$

in which $\boldsymbol{I}$ is the nth-order identity matrix, and

$$\boldsymbol{Q}_{21}(\tau) = -\frac{1}{\omega^2}\boldsymbol{M}^{-1}(\boldsymbol{K} + 2\boldsymbol{K}_2(\boldsymbol{Y}_0)+3\boldsymbol{K}_3(\boldsymbol{Y}_0)), \quad \boldsymbol{Q}_{22} = -\frac{1}{\omega}\boldsymbol{M}^{-1}\boldsymbol{C}. \tag{59}$$

Since each component of $\boldsymbol{Y}_0$ is a periodic function of τ with the period $T = 2m\pi$, each entry of $\boldsymbol{Q}_{21}$ is also a periodic function with the same period T.

The Floquet theory states that the stability criteria for the system are related to the eigenvalues of the transition matrix. The solution to Eq. (55) approaches zero as $\tau \to \infty$ if all the moduli of the eigenvalues of the transition matrix are less than 1.0; otherwise, the motion is unbounded and the solution to Eq. (31) is unstable. The way that the Floquet multipliers leave the unit circle indicates the types of bifurcations happening to the system[29].

3 Numerical results and discussion

In this work, the subharmonic resonance due to the internal resonance of the clamped-clamped buckled beam is investigated. Consider the clamped-clamped buckled beam under the base harmonic excitation with $l = 0.22\,\mathrm{m}$, $r = 15.88\,\mathrm{mm}$, $s = 0.87\,\mathrm{mm}$, $\rho = 7\,800\,\mathrm{kg/m^3}$, $E = 206.8 \times 10^9\,\mathrm{N/m^2}$, and $\widehat{c} = 0.03$. When the initial central deflection of the clamped-clamped beam is 1.56 mm with the dimensionless deflection $b = 0.007\,09$, the first linear natural frequency becomes very close to the second linear natural frequency. The first natural frequency and the ratios of the variation frequencies to the first natural frequency are shown in Table 1. Internal resonance may happen, and the energy can be transferred between the two modes. Numerical results such as nonlinear frequency and amplitude responses are provided by finding the steady-state periodic solutions obtained from the IHB method, and dynamic solutions are provided from numerical integration by using the fourth-order Runge-Kutta method. Table 2 shows the amplitudes of cosine harmonic terms with the base excitation frequency $\Omega = 75.8$ and magnitude $F = 0.199\,8$ for the numbers of retained modes $n = 2, 3, 4$, and 6, respectively. The amplitudes of cosine harmonic terms for $n = 4$ and $n = 6$ are compared. It is shown that convergence is reached when $n = 4$. Therefore, four-mode discretization is adopted in the following sections.

Table 1 First natural frequency and ratios of the first four frequencies

Dimensionless deflection b	ω_1	ω_2/ω_1	ω_3/ω_1	ω_4/ω_1
0.007 09	44.360	1.000	2.614	4.105

Table 2 Amplitudes of the cosine harmonic terms with the base excitation frequency $\Omega = 75.8$ and magnitude $F = 0.199\,8$ for different numbers of retained modes

Amplitude	Number of retained modes			
	2	3	4	6
$A_{1,1/2}$	$1.672\,2\times10^{-3}$	$1.190\,8\times10^{-3}$	$1.170\,5\times10^{-3}$	$1.170\,5\times10^{-3}$
$A_{1,1}$	$1.831\,4\times10^{-4}$	$1.287\,4\times10^{-4}$	$1.306\,1\times10^{-4}$	$1.306\,1\times10^{-4}$
$A_{2,1/2}$	$8.098\,2\times10^{-4}$	$7.896\,4\times10^{-4}$	$7.801\,1\times10^{-4}$	$7.801\,1\times10^{-4}$
$A_{2,1}$	$1.343\,0\times10^{-4}$	$1.717\,8\times10^{-4}$	$1.704\,6\times10^{-4}$	$1.704\,6\times10^{-4}$
$A_{3,1}$	–	$9.114\,3\times10^{-5}$	$9.052\,3\times10^{-5}$	$9.052\,3\times10^{-5}$
$A_{4,1}$	–	–	$1.071\,1\times10^{-5}$	$1.071\,1\times10^{-5}$
$A_{5,1}$	–	–	–	$4.893\,4\times10^{-6}$
$A_{6,1}$	–	–	–	$1.387\,6\times10^{-6}$

3.1 Nonlinear frequency response under different magnitudes of excitation

3.1.1 Case of low magnitude of excitation with $F = 0.199\,8$

Focus on the subharmonic resonance, the nonlinear frequency response of the system is discussed in the neighborhood of twice of the natural frequencies of the first two modes ω_1 and ω_2. Figures 2(a) and 2(b) show the nonlinear frequency response curves of $A_{1,1}$ and $A_{2,1/2}$ versus Ω, respectively. When the excitation frequency Ω nears $2\omega_1$ from a small value, the periodic solution is stable. Then, as the frequency sweeps to 88.15, a period-doubling bifurcation happens at Point D_1. The fundamental periodic solution is unstable with Ω is between 88.16 and 89.26. Anti-symmetric modes such as the second and fourth modes are not excited in this solution. For Period 2 solutions, there are three forms (see S_1, S_2, and S_3 in Fig. 2).

Solution S_2 comes out from the period-doubling bifurcation points D_1 and D_2. The period solutions of Y_1, Y_2, Y_3, and Y_4 can be written as follows:

$$Y_j = a_{j,0} + \sum_{k=1}^{n_c} A_{j,k/2} \cos\Big(\frac{k}{2}(\tau + \phi_{j,k/2})\Big), \quad j = 1, 2, 3, 4, \tag{60}$$

where n_c is chosen as 10 to ensure the precision. For Y_1 and Y_3, calculation shows that $A_{1,k/2}$ and $A_{3,k/2}$ are zero. Only the anti-symmetric modes contain the components of the frequency $\Omega/2$. It is found that, $a_{2,0}$, $a_{4,0}$, and $A_{j,k/2}$ ($j = 2, 4$ and $k = 2, 4, 6, \cdots$) are zero, and Y_2 and Y_4 contain only odd number harmonic components of $\Omega/2$.

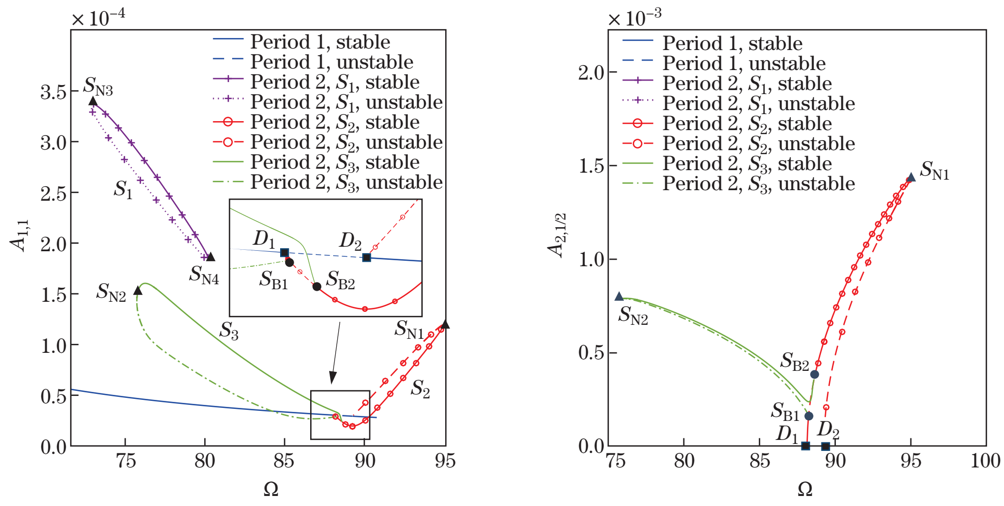

Fig. 2 Response curves of subharmonic resonance of the buckled beam with $F = 0.199\,8$ (color online)

For the second and fourth modes, the solution possesses a symmetry property. Take the second mode as an example. Its solution has the characteristic

$$Y_2(t) = -Y_2\Big(t + \frac{1}{2}T_2\Big), \tag{61}$$

where $T_2 = 4\pi/\Omega$ is the period of the second and fourth modes, which is twice of the first mode. This symmetry property is known as inversion symmetry. The response of the system is invariant under the transformation

$$(Y_1, Y_2, Y_3, Y_4) \Leftrightarrow (Y_1, -Y_2, Y_3, -Y_4), \tag{62}$$

which means if (Y_1, Y_2, Y_3, Y_4) is a solution of the system, $(Y_1, -Y_2, Y_3, -Y_4)$ can also be one.

Sweeping the excitation frequency, a part of the curves of Solution S_2 turns to be unstable at $S_{\rm B1}$ and a new branch of response is obtained. The Floquet multiplier moves outside the unit circle along the +1 direction (see Table 3), showing that a symmetry-breaking bifurcation happens in this unstable curve. Stable and unstable responses are represented by the solid and dashed lines, respectively. Unless otherwise specified, figures below will be shown in the same way. "■" denotes the period-doubling bifurcation point, and "●" and "▲" denote symmetry-breaking and saddle-node bifurcation points, respectively. For its harmonic components, the results obtained from the IHB method show that odd harmonics of the frequency $\Omega/2$ in Y_1 and Y_3 are not zero in this branch, indicating that a period-doubling phenomenon happens in the

Table 3 Floquet multipliers for bifurcation points on frequency response curves in Fig. 2

Near point	Ω	Floquet multiplier	Modulus of Floquet multiplier
D_1	89.15	−0.999 81	0.999 81
	89.16	−1.000 24	1.000 24
D_2	89.26	−1.000 23	1.000 23
	89.27	−0.999 81	0.999 81
$S_{\rm B1}$	88.24	0.997 00	0.997 00
	88.26	1.001 62	1.001 62
$S_{\rm N1}$	94.98	0.996 27	0.996 27
	94.97	1.013 12	1.013 12

first and third modes. For Y_2 and Y_4, $a_{2,0}, a_{4,0}$, and $A_{j,k/2}$ ($j = 2, 4$ and $k = 2, 4, 6, \cdots$) become nonzero, the solution components of these modes contain both odd and even harmonics of $\Omega/2$, i.e., the inversion symmetry is broken, (Y_1, Y_2, Y_3, Y_4) in this system is not invariant under the transformation in Eq. (62). The frequency response of the system exhibits the softening-spring nonlinear characteristic in Solution S_3 and the harden-spring nonlinear characteristic in Solution S_2. The amplitude of the response in Solution S_3 grows as the excitation frequency decreases. Increasing the excitation frequency can cause a change from Solution S_3 to Solution S_2. It seems that the subharmonic resonance is trapped here. Increasing or decreasing the excitation frequency does not help to stop the subharmonic resonance until it comes to the saddle-node bifurcation points $S_{\rm N1}$ and $S_{\rm N2}$. Solution S_3, which contains the subharmonic resonance in both the first and second modes, appears due to the transfer of energy from the second mode to the first mode with 1:1 internal resonance. This is similar to the investigation in Refs. [30] and [31]. Besides Solutions S_2 and S_3, there exists Solution S_1, in which subharmonic resonance is found in the first mode and the anti-symmetric modes are not excited.

3.1.2 Case of large magnitude of excitation with $F = 0.249\,7$

The magnitude of the excitation is larger in this section. Figure 3 shows the nonlinear

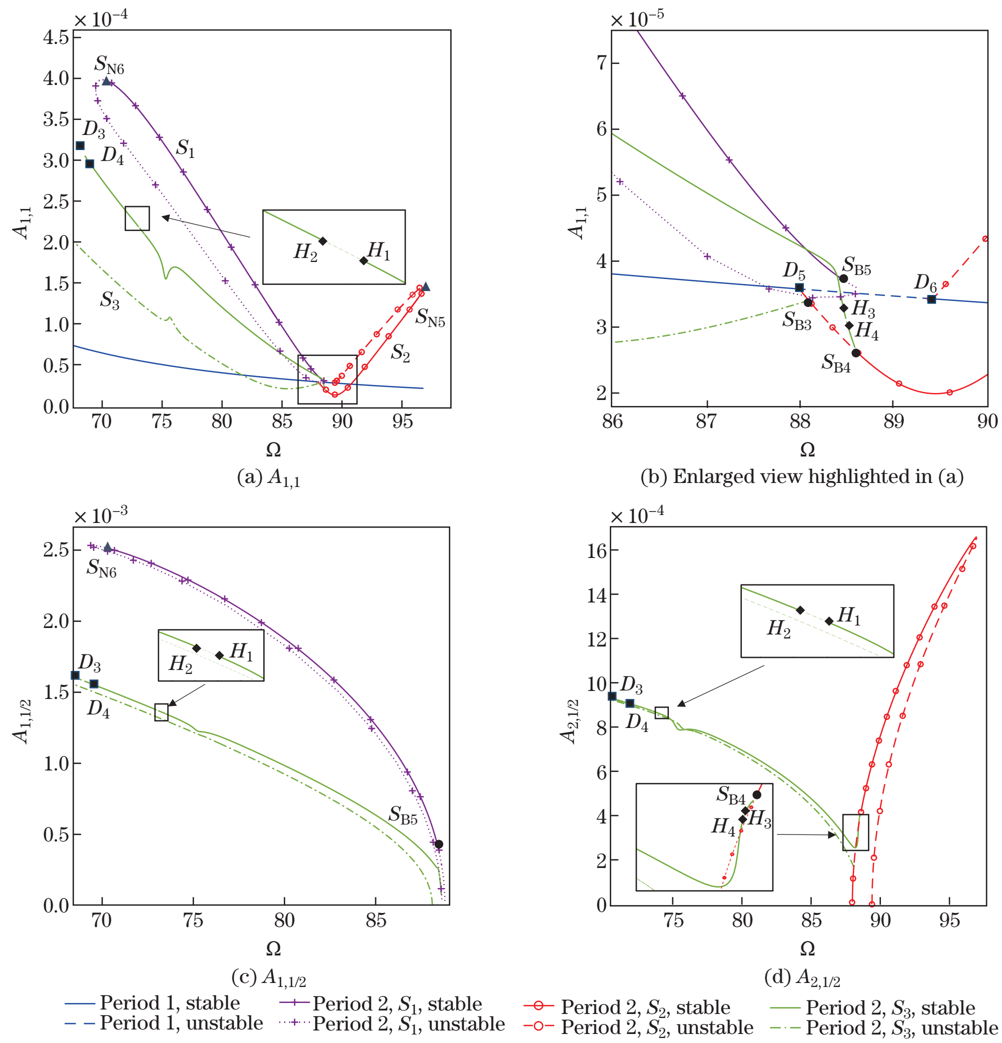

Fig. 3 Response curves of subharmonic resonance of the buckled beam with $F = 0.249\,7$ (color online)

frequency responses of $A_{1,1}$ and $A_{2,1/2}$ versus Ω. For Solution S_3, a piece of curve is found unstable between Points H_3 and H_4. The Floquet multipliers of this curve expose a Hopf bifurcation here (see "⧫"), leading to a quasi-periodic response. The numerical calculation obtained by the fourth-order Runge-Kutta method also shows the quasi-periodic motion (see Fig. 4). Figures 4(a) and 4(b) are time histories of the vibration. Figures 4(c) and 4(d) are the phase diagram of the first two modes. The Poincaré sections shown in Figs. 4(e) and 4(f) are closed curves, indicating the quasi-periodic response. The beating phenomenon is clearly shown in Figs. 4(a) and 4(b), continuously exchanging energy between the first and second modes with 1:1 internal resonance. Another Hopf bifurcation is found when $\Omega = 73.5$ (H_1) and a period-doubling bifurcation leading the solution to period-four solution occurs at Point D_4.

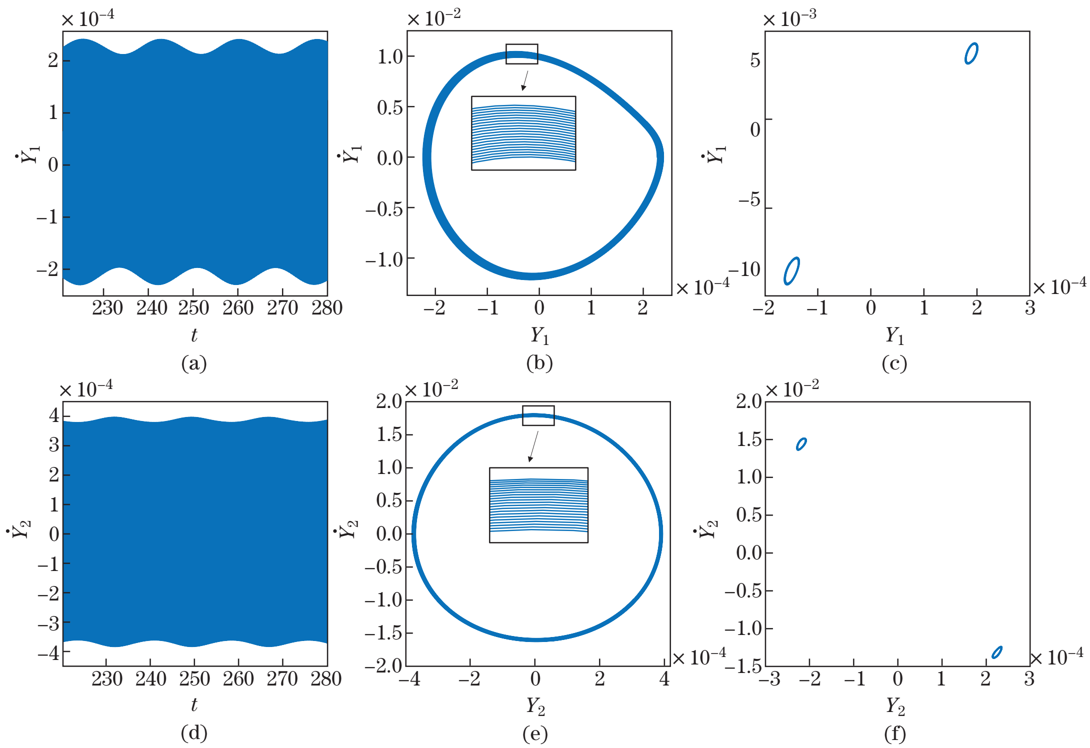

Fig. 4 Quasi-periodic response calculated by the fourth-order Runge-Kutta method with the frequency $\Omega = 88.50$ and excitation magnitude $F = 0.249\,7$. (a) and (b) are time histories of the first and second modes, (c) and (d) are phase plane diagrams, and (e) and (f) are Poincaré sections (color online)

Solution S_1 in Fig. 3 also has some change. Under higher excitation, Solution S_1 no longer exists in an isolated domain, but becomes connected with the fundamental harmonic response curve. Sweeping the excitation frequency can lead the odd components of the frequency $\Omega/2$ in Solution S_1 to zero and the solution becomes the fundamental harmonic response. It is noted that Solution S_1 cannot keep stable during this process. When it comes to Point S_{B5}, a Floquet multiplier moves outside the unit circle through $+1$, indicating that Solution S_1 jumps to Solution S_3 through this symmetry-breaking bifurcation point.

3.2 Amplitude response with the excitation frequency near twice of the first natural frequency

To investigate the subharmonic resonance, the frequency of the base excitation is set to be 88.50, which is nearly twice of the frequency of the first vibration mode. With the increase in the sweeping magnitude of the base excitation, the amplitude response of the vibration can be obtained.

Figures 5(a) and 5(b) show nonlinear amplitude response curves of $A_{1,1}$ and $A_{2,1/2}$, respectively, where blue lines denote the Period 1 solutions. When the excitation magnitude comes to 0.141 7, Period 1 response becomes unstable due to a period-doubling bifurcation happening at Point D_8 (Table 4). The Period 2 solution in the form of Solution S_2 comes out of this bifurcation point, and the solution is plotted in red with little circles. Then, Solution S_2 becomes unstable through the symmetry-breaking bifurcation point S_{B6}, and another branch of solution (S_3, plotted in green) occurs. A period-doubling phenomenon can be found in all modes, and both the even number harmonic components of frequency $\Omega/2$ in anti-symmetric modes and the odd number harmonic components of $\Omega/2$ in symmetric modes are nonzero. Solution S_3 remains stable until the base excitation magnitude comes to 0.238 5, since a Hopf bifurcation happens to Solution S_3, resulting in a quasi-periodic response via Point H_5. Solution S_3 regains its stability after Point H_6, with the excitation magnitude reaching 0.307 2. It is interesting that, with the increase in the excitation magnitude, Solution S_3 seems to be closer to Solution S_2.

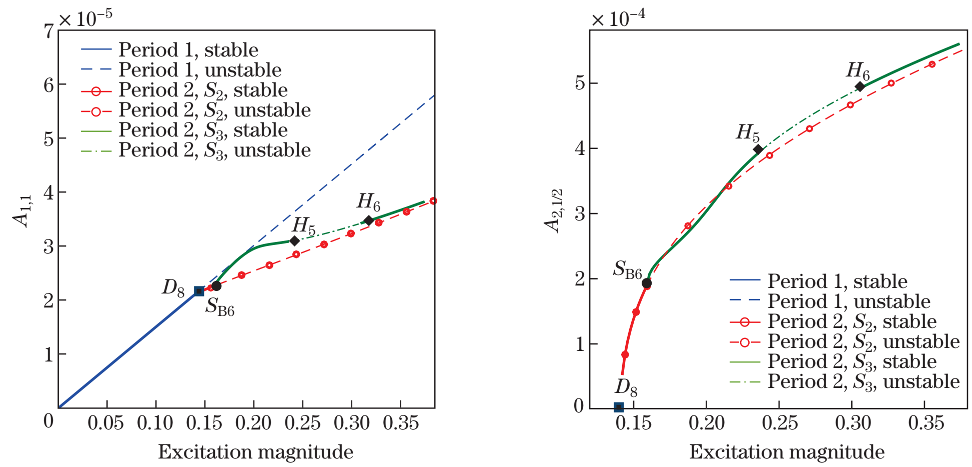

(c) $A_{1,1}$ (d) $A_{2,1/2}$

Fig. 5 Amplitude response curves of the curved beam with the base excitation frequency $\Omega = 88.50$ (color online)

Table 4 Floquet multipliers for bifurcation points on amplitude response curves in Fig. 5

Near point	F	Value of Floquet multiplier	Modulus of Floquet multiplier
D_8	0.141 1	−0.999 98	0.999 98
	0.141 7	−1.000 07	1.000 07
S_{B6}	0.177 9	0.999 39	0.999 39
	0.178 6	1.000 47	1.000 47
H_5	0.237 9	0.998 17±0.052 10i	0.999 53
	0.238 5	0.998 64±0.053 05i	1.000 05
H_6	0.306 5	0.997 07±0.079 57i	1.000 24
	0.307 2	0.996 61±0.080 11i	0.999 83

4 Conclusions

The nonlinear response and bifurcation phenomena of a clamped-clamped buckled beam system subjected to subharmonic base excitation are investigated theoretically and numerically.

The buckled beam has the property that the natural frequencies of the first and second modes are close, which results in the internal resonance under some conditions. This vibration system with quadratic and cubic nonlinearities is formulated as a four-dimensional model, and the IHB method is used to calculate the periodic solution under different base excitation frequencies and magnitudes. The Floquet theory is used to analyze the stability of the periodic solution. The time histories, phase plane diagrams, and Poincaré sections of the quasi-periodic response are treated numerically.

The results of the clamped-clamped buckled beam of 1:1 internal resonance subjected to subharmonic base excitation show that the subharmonic resonance solutions have three forms, i.e., solutions with subharmonic resonance existing in both the first and second modes, only in the first mode, and only in the second mode. The solution with subharmonic resonance only in the second mode exhibit the harden-spring nonlinearity, while the other two subharmonic resonance solutions have softening-spring nonlinearity. Sweeping the frequency of the base excitation, the form of subharmonic resonance can change, which means that once the subharmonic resonance happens via the period-doubling bifurcation, vibration at half of the excitation frequency will exist in a wide range. Moreover, bifurcations including saddle-node, Hopf, and symmetry-breaking bifurcations also occur with sweeping the excitation frequencies or magnitudes, and the quasi-periodic response is found in the investigation as well.

References

[1] HAJJAJ, A. Z., ALFOSAIL, F. K., and YOUNIS, M. I. Two-to-one internal resonance of MEMS arch resonators. *International Journal of Non-Linear Mechanics*, **107**, 64–72 (2018)

[2] TSENG, W. Y. and DUGUNDJI, J. Nonlinear vibrations of a buckled beam under harmonic excitation. *Journal of Applied Mechanics*, **38**, 467–476 (1971)

[3] ABOU-RAYAN, A. M., NAYFEH, A. H., MOOK, D. T., and NAYFEH, M. A. Nonlinear response of a parametrically excited buckled beam. *Nonlinear Dynamics*, **4**, 499–525 (1993)

[4] IBRAHIM, S. M., PATEL, B. P., and NATH, Y. Modified shooting approach to the non-linear periodic forced response of isotropic/composite curved beams. *International Journal of Non-Linear Mechanics*, **44**, 1073–1084 (2009)

[5] DING, H., ZHU, M. H., and CHEN, L. Q. Nonlinear vibration isolation of a viscoelastic beam. *Nonlinear Dynamics*, **92**, 325–349 (2018)

[6] FRATERNALI, F., SPADEA, S., and ASCIONE, L. Buckling behavior of curved composite beams with different elastic response in tension and compression. *Composite Structures*, **100**, 280–289 (2013)

[7] HUANG, J. L., SU, R. K. L., LEE, Y. Y., and CHEN, S. H. Nonlinear vibration of a curved beam under uniform base harmonic excitation with quadratic and cubic nonlinearities. *Journal of Sound and Vibration*, **330**, 5151–5164 (2011)

[8] WANG, B. Asymptotic analysis on weakly forced vibration of axially moving viscoelastic beam constituted by standard linear solid model. *Applied Mathematics and Mechanics* (*English Edition*), **33**(6), 817–828 (2012) https://doi.org/10.1007/s10483-012-1588-8

[9] WANG, Y. B., DING, H., and CHEN, L. Q. Modeling and analysis of an axially acceleration beam based on a higher order beam theory. *Meccanica*, **53**, 2525–2542 (2018)

[10] EMAM, S. A. and NAYFEH, A. H. On the nonlinear dynamics of a buckled beam subjected to a primary-resonance excitation. *Nonlinear Dynamics*, **35**, 1–17 (2004)

[11] EMAM, S. A. and NAYFEH, A. H. Non-linear response of buckled beams to 1:1 and 3:1 internal resonances. *International Journal of Non-Linear Mechanics*, **52**, 12–25 (2013)

[12] LEE, Y. Y., POON, W. Y., and NG, C. F. Anti-symmetric mode vibration of a curved beam subject to autoparametric excitation. *Journal of Sound and Vibration*, **290**, 48–64 (2006)

[13] TIEN, W. M., NAMACHCHIVAYA, N. S., and BAJAJ, A. K. Non-linear dynamics of a shallow arch under periodic excitation-I: 1:2 internal resonance. *International Journal of Non-Linear Mechanics*, **29**, 349–366 (1994)

[14] TIEN, W. M., NAMACHCHIVAYA, N. S., and MALHOTRA, N. Non-linear dynamics of a shallow arch under periodic excitation-II: 1:1 internal resonance. *International Journal of Non-Linear Mechanics*, **29**, 367–386 (1994)

[15] ÖZ, H. R. and PAKDEMIRLI, M. Two-to-one internal resonances in a shallow curved beam resting on an elastic foundation. *Acta Mechanica*, **185**, 245–260 (2006)

[16] HUANG, J. L., SU, R. K. L., LEE, Y. Y. R., and CHEN, S. H. Various bifurcation phenomena in a nonlinear curved beam subjected to base harmonic excitation. *International Journal of Bifurcation and Chaos*, **28**, 1830023 (2018)

[17] XIONG, L. Y., ZHANG, G. C., DING, H., and CHEN, L. Q. Nonlinear forced vibration of a viscoelastic buckled beam with 2:1 internal resonance. *Mathematical Problems in Engineering*, **2014**, 1–14 (2014)

[18] MAO, X. Y., DING, H., and CHEN, L. Q. Forced vibration of axially moving beam with internal resonance in the supercritical regime. *International Journal of Mechanical Sciences*, **131-132**, 81–94 (2017)

[19] LI, F. M. and YAO, G. 1/3 subharmonic resonance of a nonlinear composite laminated cylindrical shell in subsonic air flow. *Composite Structures*, **100**, 249–256 (2013)

[20] BAI, C. Q., ZHANG, H. Y., and XU, Q. Y. Subharmonic resonance of a symmetric ball bearing-rotor system. *International Journal of Non-Linear Mechanics*, **50**, 1–10 (2013)

[21] WU, F. J. and QU, L. S. Diagnosis of subharmonic faults of large rotating machinery based on EMD. *Mechanical Systems and Signal Processing*, **23**, 467–475 (2009)

[22] YANG, J. H., SANJUÁN, M. A. F., and LIU, H. G. Vibrational subharmonic and superharmonic resonances. *Communications in Nonlinear Science & Numerical Simulations*, **30**, 362–372 (2016)

[23] MAO, X. Y., DING, H., LIM, C. W., and CHEN, L. Q. Super-harmonic resonance and multi-frequency responses of a super-critical translating beam. *Journal of Sound and Vibration*, **385**, 267–283 (2016)

[24] EMAM, S. A. and NAYFEH, A. H. Nonlinear responses of buckled beams to subharmonic resonance excitations. *Nonlinear Dynamics*, **35**, 105–122 (2004)

[25] EMAM, S. A. *A Theoretical and Experimental Study of Nonlinear Dynamics of Buckled Beams*, Ph. D. dissertation, Faculty of the Virginia Polytechnic Institute and State University, Virginia, 14–21 (2002)

[26] NAYFEH, A. H., KREIDER, W., and ANDERSON, T. J. Investigation of natural frequencies and mode shapes of buckled beams. *AIAA Journal*, **33**, 1121–1126 (1995)

[27] LAU, S. L. and CHEUNG, Y. K. Amplitude incremental variational principle for nonlinear vibration of elastic systems. *Journal of Applied Mechanics*, **48**, 959–964 (1981)

[28] CHEUNG, Y. K. and LAU, S. L. Incremental time-space finite strip method for non-linear structural vibrations. *Earthquake Engineering & Structural Dynamics*, **10**, 239–253 (1982)

[29] NAYFEH, A. H. and BALACHANDRAN, B. *Applied Nonlinear Dynamics*, Wiley, New York, 187–205 (1995)

[30] IBRAHIM, S. M., PATEL, B. P., and NATH, Y. Nonlinear periodic response of composite curved beam subjected to symmetric and antisymmetric mode excitation. *Journal of Computational and Nonlinear Dynamics*, **5**, 021009 (2010)

[31] PATEL, B. P., IBRAHIM, S. M., and NATH, Y. On the internal resonance characteristics of curved beams. *Journal of Vibration and Control*, **22**, 2400–2405 (2016)